Does artificial intelligence predict elevated natriuretic peptide in chest radiography?: Emerging utilization gap for new tools

Eisuke Kagawa, MD, PhD,[1] Masaya Kato, MD, PhD,[1] Noboru Oda, MD, PhD,[1] Eiji Kunita, MD, PhD,[1] Michiaki Nagai, MD, PhD,[1] Aya Yamane, MD,[1] Shogo Matsui, MD, PhD,[1] Yuki Yoshitomi, MD,[1] Hiroto Shimajiri, MD,[1] Tatsuya Hirokawa, MD,[1] Shunsuke Ishida, MD,[1] Genki Kurimoto, MD,[1] Keigo Dote, MD, PhD[1,2]

[1] Department of Cardiology, Hiroshima City Asa Hospital, Hiroshima, Japan

[2] Department of Cardiology, Hiroshima City North Medical Centre Asa Citizens Hospital, Hiroshima, Japan

Brief title: AI, BNP, and chest X-ray

Total word count: 4299 words

Address for correspondence:

Eisuke Kagawa, MD, PhD

Department of Cardiology, Hiroshima City Asa Hospital

1-2-1, Kameyamaminami, Asakita-ku, Hiroshima, 7310293 Japan

Phone: (81) 82-815-5211

Fax: (81) 82-814-1791

E-mail: ekagawa007@gmail.com

ABSTRACT

Background and Aims: Diagnosing heart failure can be challenging. This study assessed an artificial intelligence (AI) model's performance in predicting elevated brain natriuretic peptide (BNP) levels from chest X-ray images and its potential to enhance human diagnostics.

Methods: Patients who underwent chest radiography and BNP testing on the same day were enrolled in this study. The chest X-ray images were labelled based on plasma BNP levels >= 200 pg/mL. Models were trained to predict elevated BNP levels, and the final ensemble model was constructed. Humans were tested to predict elevated BNP levels, followed by the same test, referring to the AI model's predictions. The diagnostic performance was evaluated.

Results: Among the 1607 patients, 10103 images and BNP values were collected. The AI model achieved an accuracy of 0.855, precision of 0.873, sensitivity of 0.827, receiver-operating-characteristics area-under-curve of 0.929 with the test dataset. The accuracy of the testing with the 100 images by 35 individuals significantly improved from 0.708±0.049 to 0.829±0.069 ($P < 0.001$) with the AI model' assistance, which had an accuracy of 0.920. The accuracy of the experts was higher than that of non-experts (0.692±0.042 vs. 0.728±0.051, $P = 0.030$); however, with the AI assistance, the accuracy of the non-experts was rather higher than that of the experts (0.851±0.074 vs. 0.803±0.054, $P = 0.033$).

Conclusions: The AI model can predict elevated BNP levels from chest X-ray images and has the potential to improve human diagnostic performance. The gap in utilizing new tools represents one of the emerging issues.

Keywords: deep learning, neural network, machine learning, brain natriuretic peptide, heart

failure, image recognition

Introduction

Heart failure is one of the major causes of visits to medical facilities in both unplanned emergency situations and routine medical checkups. It is also a growing and called heart failure pandemic because of the aging population.[1,2] However, diagnosing heart failure, which should be medically managed, can be challenging due to the variability of symptoms, especially in heart failure that is complicated by other diseases for patients visiting medical facilities or for attending physicians who are not familiar with cardiovascular disease.[3] Several tests are used to evaluate heart failure.[1,2] Chest X-rays are widely available, and the images can be obtained quickly; however, the evaluation of chest X-ray images requires experience and has limited sensitivity and specificity for heart failure.[4] Natriuretic peptide is useful for evaluating heart failure not only in emergency situations for diagnosis but also for heart failure management.[5-7] However, natriuretic peptide testing requires equipment, and even if the facility has such equipment, it may not be available at all hours, as many facilities do not offer testing at night or on weekends. Furthermore, it is essential to make the decision to perform the test itself. We hope that automated support tools will be developed to assist in our daily practice of heart failure quickly and inexpensively. The rise of artificial intelligence (AI) and the evolution of computer hardware provide novel findings and solutions.[8,9] With regard to image recognition, deep neural networks (deep learning) provide relatively good performance compared to those of previous architectures, and some of them can be utilized in the real clinical world.[10-13] The aim of our study was to diagnose heart failure using chest X-ray imaging and an AI model, and to support clinical practice. We assessed the hypothesis that AI models that predict elevated brain natriuretic peptide (BNP) levels from chest X-ray images could provide excellent performance compared to experienced cardiologists and could improve the diagnostic performance of humans.

Methods

Study Patients and Datasets

Patients who underwent chest radiography and BNP testing on the same day at Hiroshima City Asa Hospital and Hiroshima City North Medical Centre Asa Citizens Hospital from October 2021 to September 2022 were eligible for this study. Since BNP testing is the first choice for natriuretic peptide testing in these hospitals, and not N-terminal pro-brain natriuretic peptide, we selected BNP for this study. We reviewed the medical records of eligible patients, including periods other than the above, and when chest X-ray and BNP testing were performed on the same day, the chest X-ray images, and plasma BNP values were collected. To increase the robustness and generalizability of the AI models, all conditions of the frontal view of chest X-ray images were collected, including anterior-posterior, posterior-anterior, standing, sitting, and supine positions, with or without inspiration, and any diseases or conditions. Lateral chest radiographs were not included in this study. Patients taking an angiotensin receptor neprilysin inhibitor were included because we intended to make models robust and widely available in real clinical settings, and it might not increase BNP.[14] According to the statement of the Japanese Heart Failure Society, we used a BNP cut-off value of 200 pg/mL for the main study and 100 pg/mL for the sub study.[15] The chest X-ray images were labelled binary according to the cut-off value. The patients from Hiroshima City Asa Hospital were used for the training and validation datasets, while the patients from Hiroshima City North Medical Centre Asa Citizens Hospital were used for the test dataset. The study patients from Hiroshima City Asa Hospital were randomly divided into two datasets for training and validation. The patients were assigned to datasets in the training: validation: testing dataset ratio of approximately 0.66:0.17:0.17. Many patients had

multiple pairs of chest X-ray images and BNP labels, and each patient's data were assigned to only one dataset to avoid overfitting. The patients who were duplicated in both hospitals were assigned to only one dataset. The study was approved by the local institutional review board.

Image Pre-processing

Non-square chest X-ray images were transformed to square using 0 padding (black field), not cropping. We planned to pre-process the images in which the head was in the upper half of the image and the spine was at 60 ° - 120 ° angle to the horizontal line of images. However, all the images met these requirements, so these image pre-processing steps were not utilized.

Outline of an AI Model

We designed AI models to predict higher BNP levels as follows: First, as weak learners, we fine-tuned 31 modified pre-trained image recognition models. The bias of the models was checked using a featured map of gradient-class activation maps (GRAD-CAM) or attention maps. If the model strongly focused on irrelevant objects for the classification, we discarded it and retrained a new model until the model no longer focused on them. Second, we created a soft ensemble prediction model using the weak learners. Details of training for models are provided in the Supplemental Methods.

Evaluation of Models

After obtaining the 31 models (weak learners), we constructed the final soft ensemble model by averaging the probabilities of the 31 models. Probabilities >= 0.5 were considered to represent BNP levels >= the cut-off value. The accuracy, precision, sensitivity (recall), specificity, F1 score,

receiver-operating-characteristics (ROC) curves, and precision-recall (PR) curves were calculated using the test dataset. ROC and PR curves were constructed using probability of BNP >= cut-off value, and the area under the curve (AUC) was calculated. To avoid overfitting the test dataset, the results of the performance tests using the test dataset were not used to retrospectively train or select the models.

Human Testing

We evaluated human performance to predict elevated BNP levels from chest X-ray images. The subjects were voluntary participants from the hospital staff. The general findings of heart failure seen in chest X-ray images, as well as the characteristics of BNP, were taught to those being tested. The test subjects were shown chest X-ray images and their corresponding BNP labels in the training dataset for their learning phase. Then, they evaluated the 100 chest X-ray images from the test dataset and provided their binary prediction. The 100 images for human testing comprised 50 images with BNP < the cut-off value and 50 with BNP >= the cut-off value, presented in random order. After the first test, to assess whether the AI assistance could improve human diagnostic performance, the test subjects evaluated the same 100 images again, this time with reference to the predictions of the AI model. The performance of the AI model, which had the accuracy of 86% on the test dataset (approximately 10 to 20% higher than that of humans), was explained before the second test. The accuracy of the AI model for the 100 images and the ratio of the two labels were not disclosed to the test subjects until all tests were completed. An expert was defined as someone with a medical career of >= 10 years.

Sub Study

We developed models to predict the BNP values. Images with BNP values >= 2000 pg/mL were excluded from the three datasets; the top two full connected layers were replaced with three full connected layers (two layers of 1024 neurons with activation function mish and one layer with one neuron with sigmoid function). We trained the models using the last 11 layers, which are trainable for fine-tuning. Additionally, we trained models to predict elevated BNP values with a cut-off of 100 pg/mL, modifying hyperparameters based on the training from the main study.

Statistical Analysis and Calculations

Continuous variables are presented as medians (with first and third quartiles) or as mean ± standard deviation (SD), and categorical variables are presented as numbers and percentages, as appropriate. We utilized Python 3.10.7 (Python Software Foundation, Delaware, USA) and TensorFlow 2.10.1 (Google LCC, Mountain View, CA, USA) for our machine learning and statistical analysis.[16] The models were trained using an NVIDIA GeForce RTX 3080Ti GPU (NVIDIA Corporation, Santa Clara, CA, USA) or the Google Colaboratory platform (Google LLC, Mountain View, CA, USA). The difference in the accuracies of the first and second human tests was tested using Welch's t-test or paired t-test, as appropriate. A P value < 0.05 was considered statistically significant.

Results

Baseline Characteristics

An overview of this study is shown in Figure 1, and the baseline characteristics of the study patients are shown in Table 1. Among the 1607 patients in the study, the diagnoses included heart failure (N = 471), acute heart failure (N =320), coronary artery disease (N = 517), acute coronary

syndrome (N = 176), hypertrophic cardiomyopathy (N = 32), interstitial pneumonia (N = 64), and haemodialysis (N = 23). In total, 10103 chest X-ray images were collected. These images were divided among the training, validation, and test datasets as follow: 1061 patients (66%) with 6697 images (66%), 273 patients (17%) with 1693 images (17%), and 273 patients (17%) with 1713 images (17%).

Performance of the AI

The 31 models (weak learners) were created and trained (Figure 2). Their performance is detailed in Table 2, Figure 3, and the Structured Graphical Abstract. The performance metrics of the final ensemble model were as follows: accuracy was 0.855, precision was 0.873, sensitivity (recall) was 0.827, specificity was 0.882, F1 score was 0.850, ROC AUC was 0.929, and PR AUC was 0.934.

Performance of Human

A total of 35 individuals, including 20 medical doctors of whom 13 were cardiologists, were tested using the 100 images. The duration of medical practice among the participants was 10.2±9.0 years, with 16 identified as experts. The AI model's performance on the 100 images was as follows: the accuracy 0.920, sensitivity 0.880, specificity 0.957, and f1 score 0.917 (Structured Graphical Abstract). Without the AI assistance, the human participants achieved an accuracy of 0.708±0.049, a sensitivity of 0.693±0.128, and a specificity of 0.722±0.144. With the AI assistance, these measures significantly improved to an accuracy of 0.829±0.068 ($P < 0.001$) (Figure 4 and Structured Graphical Abstract), a sensitivity of 0.787±0.113, and a specificity of 0.872±0.097. Even with the AI assistance, no human subjects surpassed the performance of the

AI model in terms of accuracy, precision, specificity, or f1 score. The accuracy of the medical doctors and experts was higher than that of non-medical doctors and non-experts in the non-assisted test, respectively (0.687±0.032 vs. 0.725±0.054, P = 0.014; 0.692±0.042 vs. 0.728±0.051, P = 0.030). However, with the AI assistance, the accuracy of the medical doctors was similar to that of the non-medical doctors (0.843±0.074 vs. 0.818±0.064, P = 0.289), and the accuracy of the non-experts was even higher than that of the experts (0.851±0.074 vs. 0.803±0.054, P = 0.033) (Structured Graphical Abstract, Figure 5). In the AI-assisted test, there were 3 non-experts and 1 expert who responded entirely based on the AI model's predictions, and these four participants achieved the highest accuracy throughout the test, with an accuracy of 0.920. In the non-assisted test, the accuracy had a weak positive correlation with the duration of medical careers (r = 0.414, P = 0.014), while in the AI-assisted test it showed a weak negative correlation (r = -0.347, P = 0.041). For the eight images that were incorrectly predicted by the AI model, the human accuracy was 0.301±0.124. For the hard ensemble prediction by the humans using majority voting, accuracy was 0.800 with the first test and 0.880 with the AI assistance.

Sub Study

We developed a model to predict BNP values. The mean absolute errors (MAE) between the predicted and true BNP values were 208 pg/mL for the weak learners, with mean squared errors being $1.01*10^5$ pg^2/mL^2. No significant difference was observed between the predicted and true BNP values (P = 0.274). The models' performances in predicting elevated BNP level using a cut-off of 100 pg/mL was comparable to that of the models using a cut-off of 200 pg/mL (Table 2, Figure 3).

Discussion

This study presents the development of a high-performing model that predicts elevated BNP levels from chest X-ray images, thereby improving human diagnostic accuracy.

The strengths of our study are as follows: First, this is the first report demonstrating that an AI model can predict elevated BNP levels from chest X-ray images, outperforming experienced cardiologists. Our models were predicated on the hypothesis that chest X-ray images contain features associated with elevated BNP levels indicative of heart failure. Prior reports have associated chest X-ray findings such as cardiomegaly, pulmonary venous congestion, interstitial or alveolar oedema, and cephalization with heart failure prediction.[2,4] Cephalization and interstitial and alveolar oedema are reported to be modestly specific for heart failure, albeit not very sensitive (sensitivity of 47 – 61% for elevated pulmonary capillary wedge pressure). These prior evaluations were human based; our study establishes superior diagnostic performance by the AI models in predicting elevated BNP levels, substantiating the one of our hypotheses. The featured map images revealed that our models capture chest X-ray findings akin to prior human reports on chest radiography and heart failure (Figure 2). Nevertheless, various factors such as age, sex, haemoglobin level, renal function, left ventricular end-diastolic pressure, and left ventricular ejection fraction influence plasma BNP levels, so BNP level cannot be perfectly evaluated solely through chest X-ray imaging.[17] Conversely, the predictability, as indicated by the ROC AUC, was above 0.929 in our test dataset population, suggesting a high level predictability. Matsumoto et al. reported that transfer-learned VGG16 models predict heart failure from the chest X-ray images labelled by two cardiologists.[18] A limitation of their study was the diagnosis of heart failure by two cardiologists. Our study highlights the relative inferiority of physician performance in predicting elevated BNP levels compared to the AI model,

even among experienced cardiologists. Other reports have showed that chest radiography can predict pulmonary hypertension or elevated pulmonary artery wedge pressure.[19,20] One limitation of their study is the difference in timing between when the catheterization was performed and when the X-ray was taken, as the pulmonary artery pressure can greatly vary depending on the patient's condition such as posture. Additionally, the relatively low predictive performance could be attributed to the small sample size. Zou et al. reported that their model predicted pulmonary hypertension from a chest X-ray image with an ROC AUC of 0.967; however, their models were trained and tested in selected images that excluded several conditions such as pleural/pericardial effusion, pneumothorax, pulmonary atelectasis, and massive consolidation obstruction of the right ventricular outflow tract, or pulmonary artery were excluded. In contrast, our study included all available chest X-ray images, encompassing a broad spectrum of conditions such as trauma, interstitial pneumonia, mechanically ventilated patients, respiratory failure, implanted cardiac devices, dextrocardia, congenital heart diseases, dialysis, and hypertrophic cardiomyopathy, in addition to conditions excluded in the aforementioned studies, suggesting our model's robustness.

Second, the performance of our models was benchmarked against front-line physicians. Although numerous AI studies have reported that the AI models could accurately predict medical features from conventional tests, many of these did not evaluate the performance of physicians. Our study demonstrated that not only the ensemble models, but also the individual weak learners outperformed experienced physicians, and it highlighted the performance of non-experts in diagnosing elevated BNP levels.

Third, we showed that the AI model's suggestions could enhance human diagnostic performance, and the utilization gap for new tools is an emerging issue. Regardless of the

superior performance of a support tool, it is useless if it is not trusted or utilized by users. To date, there have been no reports indicating that AI model assistance improve human diagnostic performance. Previous reports on medical prediction models focused exclusively on the performance of the models themselves. This study discovered that performance was positively associated with the duration of medical careers. However, AI assistance improved the diagnostic performance of both inexperienced and experienced practitioners, with the inexperienced ones achieving similar or even surpass experienced ones. This implies that with the aid of a potent diagnostic tool, inexperienced individuals can perform as well as or even surpass experienced ones. The limited improvement among the experts may be attributed to their confidence in their expertise and scepticism towards the AI model, despite being informed of the AI model's superior performance compared to any human. Conversely, a less experienced individual might readily accept the AI's prediction due to lack of confidence. Distrust in new technology or findings and self-confidence will be emerging issues in AI; this kind of scepticism towards novel approaches has always existed in other domains. In particular, the usage of generative AI has begun to be actively discussed. We must strive to understand and adapt appropriately to new ideas, technologies, tools, and methods, including AI.

Fourth, the models utilized in this study, along with the sample codes for their usage, will be made available on GitHub after the publishment. This implies that anyone can test and refine the models, and challenge old notions with new ideas.

Fifth, we enhanced the models using a variety of techniques. Apart from traditional standard methods like data augmentation with shift, flip, and rotations, "relu" activation function, "Adam" optimizer, and convolutional layers, our model was designed to incorporate current or past state-of-the-art techniques. These included data augmentations of MixUp, Random Erasing, and

Cutmix, “mish” activation function, label smoothing regularization, sharpness aware minimization optimizer, non-convolutional layer architectures such as vision transformer and MLP-mixer, and model refinement to control bias using featured maps. Finally, an ensemble of these models was utilized to create the strong learner. Our models were based on these technical aspects, and our collected dataset, which was comprehensive and had not been used in previous reports regarding heart failure and chest X-ray, is thought to be one of the strengths of our study and may enhance the model’s robustness and generalizability.

Sixth, traditional chest radiographs are widely available in medical facilities. Though these AI models are relatively large and require time to train even using graphics processing unit, binary predictions from a single image can be performed in a short period. If we do not use ensembles, or if we minimize the number of ensembles, we can make predictions even faster. Technically, it is not difficult to integrate this software into smartphones or X-ray machines. Further advancements in both hardware and software could simplify this process even more, allowing these tools to be used in an increasingly diverse manner, potentially changing the world.

Ensemble prediction has the potential to improve performance.[21] In our study, we utilized soft voting, which improved the performance from the single models (weak leaners), with an accuracy of 0.818 to the ensemble model accuracy of 0.855. For instance, with the ensemble method and three weak learners implementing simple majority voting for binary prediction, the ensemble’s decision will be correct if more than two weak learners predict accurately. Assuming each weak learner to be independent and their probability uniformly 0.8, the probability that more than two weak learners are correct is 0.896 (0.8 * 0.8 * 0.8 + 0.2 * 0.8 * 0.8 * 3). To enhance the performance of the ensemble, the models’ performances should be reasonably good and their prediction correlation should not be overly strong. This parallels the performance of a

heart team, where members who consistently agree with others, or remain silent, contribute little to the quality of decisions, and active members lacking a certain level of performance can impair overall performance. Concerning an ensemble model, weak learners should be different from each other because the correlation should not be extremely high, even though we intended to train all models in the best possible way. Given that sensitivity and specificity exist in a trade-off relationship, a weak learner that may not be the best in terms of overall accuracy could potentially enhance the accuracy and generalizability of the ensemble model due to the diversity it provides. Approaches to improve ensemble model accuracy may include replacing less accurate learners with more accurate models, adding more accurate models to the ensemble, or selecting or retraining weak learners based on ensemble performance. However, we avoided these approaches as they led to overfitting to the test dataset, compromising generalizability and robustness, and ultimately degrading performance. This illustrates one of the challenges of implementing ensemble methods. Given that the correlation of models' predictions remains unknown until the completion of model training, we cannot predict the models' performance or determine optimal hyperparameters for deep learning in advance. We cannot foresee the results; we can only make sense of the retrospectively. Therefore, we must trust that the weak learners will contribute to improved performance in the future and train them using a variety of sophisticated methods, analogous to human education.

Study Limitations

The accuracy of the models was influenced by the proportion of images in the test dataset that were difficult to diagnose. When evaluating with a different dataset, wherein the proportion of such difficult images derivates from that of our test dataset, the accuracy could diverge from our

study results. Nevertheless, as our dataset was collected from daily clinical practice and is representative of all-comers, we expect it to exhibit a certain level of generalizability and robustness. In the sub study predicting absolute BNP values, no statistical difference was observed between the predicted and true BNP value. However, the MAE was 208 pg/mL, approximately the same as the cut-off for BNP in this study, which did perform as well as the binary prediction of BNP levels. This may be partially due to sample size, and performance could potentially improve with a larger dataset. Natriuretic peptides are used for diagnosis of heart failure, employing either absolute values or relative changes, and for managing the condition through sequential relative changes. This study primarily conducted with binary prediction, as the main goal was to diagnose heart failure in this time. The clinical impact of the discrepancies between the predicted and true BNP values might depend on their application in clinical settings. Notably, the human performance in predicting absolute BNP values from chest X-ray images was extremely poor in preliminary testing (data not shown). The choice of a cut-off BNP value warrants discussion. The cut-off values should be determined based on intended purpose while ensuring a balance between sensitivity and specificity. We set the BNP cut-off value at 200 pg/ml with the aim of diagnosing unrecognized heart failure that requires early management; however, a cut-off value of 100 or 125 pg/ml would be considered for different purposes or applications. In this study, models with a cut-off of 100 pg/ml demonstrated performance comparable to those with a cut-off of 200 pg/ml. While we labelled the X-ray images based on the BNP cut-off value, it is important to remember that heart failure is not diagnosed based solely on natriuretic peptide values. One of our goals is to diagnose unrecognized heart failure that needs early intervention, which is not synonymous with diagnosing elevated BNP levels alone.

Conclusions

The AI model can predict elevated BNP levels from chest X-ray images with superior performance compared to experienced cardiologists and can improve the diagnostic performance of individuals, ranging from non-experts to experienced cardiologists. These models may be useful in clinical settings. The gap in utilizing new tools represents one of the emerging issues.

Acknowledgements

We express our gratitude to all the individuals who participated in this study.

Funding

There is no financial support for this study.

Conflict of interest

There are no conflicts of interest.

Data availability statement

Data sharing requests will be considered upon a reasonable request to the corresponding author. The models used in this study, along with the sample code for their utilization, will be made available on GitHub following the publication of this study.

References

1. McDonagh TA, Metra M, Adamo M, *et al.* 2021 ESC Guidelines for the diagnosis and treatment of acute and chronic heart failure. *Eur Heart J* 2021;**42**:3599-3726. doi: 10.1093/eurheartj/ehab368

2. Heidenreich PA, Bozkurt B, Aguilar D, *et al.* 2022 AHA/ACC/HFSA Guideline for the Management of Heart Failure: A Report of the American College of Cardiology/American Heart Association Joint Committee on Clinical Practice Guidelines. *Circulation* 2022;**145**:e895-e1032. doi: 10.1161/cir.0000000000001063

3. Stevenson LW, Perloff JK. The limited reliability of physical signs for estimating hemodynamics in chronic heart failure. *JAMA* 1989;**261**:884-888. doi:

4. Chakko S, Woska D, Martinez H, *et al.* Clinical, radiographic, and hemodynamic correlations in chronic congestive heart failure: conflicting results may lead to inappropriate care. *Am J Med* 1991;**90**:353-359. doi: 10.1016/0002-9343(91)80016-f

5. Maisel AS, Krishnaswamy P, Nowak RM, *et al.* Rapid measurement of B-type natriuretic peptide in the emergency diagnosis of heart failure. *N Engl J Med* 2002;**347**:161-167. doi: 10.1056/NEJMoa020233

6. Mueller C, Scholer A, Laule-Kilian K, *et al.* Use of B-type natriuretic peptide in the evaluation and management of acute dyspnea. *N Engl J Med* 2004;**350**:647-654. doi: 10.1056/NEJMoa031681

7. McLellan J, Bankhead CR, Oke JL, *et al.* Natriuretic peptide-guided treatment for heart failure: a systematic review and meta-analysis. *BMJ Evid Based Med* 2020;**25**:33-37. doi: 10.1136/bmjebm-2019-111208

8. van Smeden M, Heinze G, Van Calster B, *et al.* Critical appraisal of artificial

intelligence-based prediction models for cardiovascular disease. *Eur Heart J* 2022;**43**:2921-2930. doi: 10.1093/eurheartj/ehac238

9. Gill SK, Karwath A, Uh HW, *et al.* Artificial intelligence to enhance clinical value across the spectrum of cardiovascular healthcare. *Eur Heart J* 2023;**44**:713-725. doi: 10.1093/eurheartj/ehac758

10. Krizhevsky A, Sutskever I, Hinton GE. Imagenet classification with deep convolutional neural networks. *Advances in neural information processing systems* 2012;**25**. doi:

11. Attia ZI, Noseworthy PA, Lopez-Jimenez F, *et al.* An artificial intelligence-enabled ECG algorithm for the identification of patients with atrial fibrillation during sinus rhythm: a retrospective analysis of outcome prediction. *Lancet* 2019;**394**:861-867. doi: 10.1016/s0140-6736(19)31721-0

12. Gessert N, Lutz M, Heyder M, *et al.* Automatic Plaque Detection in IVOCT Pullbacks Using Convolutional Neural Networks. *IEEE Trans Med Imaging* 2019;**38**:426-434. doi: 10.1109/tmi.2018.2865659

13. Wouters PC, van de Leur RR, Vessies MB, *et al.* Electrocardiogram-based deep learning improves outcome prediction following cardiac resynchronization therapy. *Eur Heart J* 2023;**44**:680-692. doi: 10.1093/eurheartj/ehac617

14. Myhre PL, Prescott MF, Murphy SP, *et al.* Early B-Type Natriuretic Peptide Change in HFrEF Patients Treated With Sacubitril/Valsartan: A Pooled Analysis of EVALUATE-HF and PROVE-HF. *JACC Heart Fail* 2022;**10**:119-128. doi: 10.1016/j.jchf.2021.09.007

15. The Japanese Heart Failure Society Committee on Heart Failure Prevention, Sato Y, Yoshimura M, *et al.* Guidelines regarding management for heart failure using blood BNP and NT-proBNP levels. http://www.asas.or.jp/jhfs/english/outline/guidelines_20180822.html (March

31 2023)

16. Kluyver T, Ragan-Kelley B, Pérez F, *et al*. Jupyter Notebooks-a publishing format for reproducible computational workflows; 2016.

17. Tsutamoto T, Wada A, Sakai H, *et al.* Relationship between renal function and plasma brain natriuretic peptide in patients with heart failure. *J Am Coll Cardiol* 2006;**47**:582-586. doi: 10.1016/j.jacc.2005.10.038

18. Matsumoto T, Kodera S, Shinohara H, *et al.* Diagnosing Heart Failure from Chest X-Ray Images Using Deep Learning. *Int Heart J* 2020;**61**:781-786. doi: 10.1536/ihj.19-714

19. Zou XL, Ren Y, Feng DY, *et al.* A promising approach for screening pulmonary hypertension based on frontal chest radiographs using deep learning: A retrospective study. *PLoS One* 2020;**15**:e0236378. doi: 10.1371/journal.pone.0236378

20. Hirata Y, Kusunose K, Tsuji T, *et al.* Deep Learning for Detection of Elevated Pulmonary Artery Wedge Pressure Using Standard Chest X-Ray. *Can J Cardiol* 2021;**37**:1198-1206. doi: 10.1016/j.cjca.2021.02.007

21. Lam L, Suen SY. Application of majority voting to pattern recognition: an analysis of its behavior and performance. *IEEE Transactions on Systems, Man, and Cybernetics - Part A: Systems and Humans* 1997;**27**:553-568. doi: 10.1109/3468.618255

Legends

Structured Graphical Abstract:

We developed the AI model to predict elevated BNP levels using 31 weak learners. The AI model achieved an accuracy of 0.920, sensitivity of 0.880, and specificity of 0.957 with the 100 images. The accuracy of the testing with the 100 images by 35 individuals significantly improved from 0.708±0.049 to 0.829±0.069 ($P < 0.001$) with the AI model' assistance. The accuracy of the experts was higher than that of non-experts (0.692±0.042 vs. 0.728±0.051, $P = 0.030$); however, with the AI assistance, the accuracy of the non-experts was rather higher than that of the experts (0.851±0.074 vs. 0.803±0.054, $P = 0.033$). AI, artificial intelligence; AUC, area-under-curve; BNP, brain natriuretic peptide.

Figure 1: Overview of the study. We designed AI models to predict higher BNP levels as follows: First, as weak learners, we fine-tuned 31 modified pre-trained image recognition models. The bias of the models was checked using a featured map of GRAD-CAM or attention maps. If the model strongly focused on irrelevant objects for the classification, we discarded it and retrained a new model until the model no longer focused on those objects. Second, we created a soft ensemble prediction model using the weak learners. For human testing, the examinee was presented with chest X-ray images and their corresponding BNP labels from the training dataset for learning purposes. The examinee then evaluated 100 chest X-ray images from the test dataset and provided binary predictions. Following the initial test, the examinee reassessed the same 100 images, referring to the predictions made by the AI model, to determine if the AI assistance could improve human diagnostic performance. AI, artificial intelligence; AUC, area-under-curve; BNP, brain natriuretic peptide; GRAD-CAM, gradient-class activation maps; GPU, graphic processing

unit; PR, precision-recall; ROC, receiver-operating-characteristics.

Figure 2: Chest X-ray images and featured map of weak learners. **(A**) Chest X-ray image with a BNP of 9 pg/mL and a GRAD-CAM image generated by the EfficientNetV2L-based-model. (**B**) The EfficientNetV2L-based-model identified features such as pulmonary congestion and pacemaker, with a BNP of 798 pg/mL. (**C**) The attention map revealed the Vit-b16-based-model's features in the caption, the pulmonary vessel, and the diaphragmatic line, with a BNP of 413 pg/mL. The caption in the upper left corner is a Kanji character meaning the supine position. (**D**) The EfficientNetV2S-based-model identified features in the captions of images with a BNP of 824 pg/mL. The caption in the upper left corner is a Kanji character meaning the sitting position. (**E**) The model utilized in (**D**) was retrained, and the new model did not focus on the features in the captions but on the pleural effusion, cardiomegaly, pulmonary artery, air bronchogram, and Kerley A lines. The caption in the upper left corner is a Kanji character meaning the sitting position. BNP, brain natriuretic peptide; GRAD-CAM, gradient-class activation maps.

Figure 3: Performance of the models. The ROC curves (A) and PR curves (B) of the AI models for predicting BNP >= 200 pg/ml are shown. Similarly, the ROC curves (C) and PR curves (D) for predicting BNP >= 100 pg/ml are shown. The ROC and PR curves were shown for the final ensemble model as well as for 3 of the 31 weak leaners. BNP, brain natriuretic peptide; PR, precision recall; ROC, receiver-operating-characteristics.

Figure 4: Representative images and predictions of the AI models and humans. The chest X-ray

images and their featured map images, age, sex, BNP value, AI prediction, and human accuracy are shown. The featured map images were generated by the EfficientNetV2S-based-model using GRAD-CAM. The caption in the upper right corner of (**A**) and the upper left corner of (**B, C, and D**) are Kanji character meaning sitting and standing position, respectively. AI, artificial intelligence; BNP, brain natriuretic peptide; GRAD-CAM, gradient-class activation maps. AI, artificial intelligence; BNP, brain natriuretic peptide; GRAD-CAM, gradient-class activation maps.

Figure 5: The accuracy of the humans' testing. **(A and B)** Both the non-experts (0.692±0.042 vs. 0.851±0.074, $P < 0.001$) and experts (0.728±0.051 vs. 0.803±0.054, $P < 0.001$) improved their accuracy with the assistance of the AI model. **(C)** The increase in the accuracy with the AI assistance was greater for the non-experts than for the experts (0.159±0.069 vs. 0.074±0.052, $P < 0.001$). **(D)** In the non-assisted test, the accuracy had a weak positive correlation with the duration of medical careers ($r = 0.414$, $P = 0.014$). **(E)** However, in the AI-assisted test, it had a weak negative correlation ($r = -0.347$, $P = 0.041$). AI, artificial intelligence.

Table 1. Characteristics of the Study Patients and Materials

Patient	
Study patients	1607
Male sex	980 (61)
Diagnosis (multiple)[a]	
Heart failure	471 (29)
Acute heart failure	320 (20)
Coronary artery disease	517 (32)
Acute coronary syndrome	176 (11)
Hypertrophic cardiomyopathy	32 (2)
Congenital heart disease	14 (1)
Atrial fibrillation	253 (16)
Peripheral artery disease	97 (6)
Pericardial effusion	6 (1)
Aortic disease	68 (4)
Haemodialysis	23 (1)
Chronic kidney disease	171 (11)
Pneumonia	62 (4)
Interstitial pneumonia	64 (4)
Venous thromboembolism	43 (3)
Pneumothorax	9 (1)
Lung carcinoma	16 (1)
Trauma	5 (1)

Chest pain syndrome	29 (2)
Dataset, patients	
Train	1061 (66)
Valid	273 (17)
Test	273 (17)
Images	
Chest X-ray images, N	10103
Age, y	74 (64 – 81)
Plasma BNP, pg/ml	158 (47 – 569)
Dataset, images	
Train	6697 (66)
BNP >= 200 pg/ml	2994 (45)
Valid	1693 (17)
BNP >= 200 pg/ml	726 (43)
Test	1713 (17)
BNP >= 200 pg/ml	852 (50)

Data presented as N (%) or median (interquartile range).

BNP, brain natriuretic peptide.

[a] Multiple selections were allowed to account for patients with co-existing conditions.

Table 2. Performance of Models with BNP Cut-Off as 200 pg/ml

Model [a]	**Input size**	**Accuracy**	**Precision**	**Sensitivity (Recall)**	**Specificity**	**F1 score**	**ROC AUC**	**PR AUC**
BNP Cut-off: 200 pg/ml (main study)								
VGG16	224	0.842	0.868	0.805	0.879	0.835	0.919	0.926
VGG16	384	0.823	0.877	0.749	0.897	0.808	0.907	0.914
VGG19	224	0.838	0.869	0.793	0.882	0.829	0.913	0.918
VGG19	384	0.841	0.871	0.799	0.883	0.833	0.915	0.923
VGG19_2	384	0.834	0.844	0.816	0.852	0.830	0.910	0.917
InceptionResNetV2	299	0.829	0.852	0.793	0.864	0.822	0.909	0.909
Xception	299	0.791	0.916	0.638	0.942	0.752	0.899	0.904
Xception_2	299	0.840	0.862	0.807	0.873	0.834	0.919	0.926
MobileNetV3Small	224	0.809	0.876	0.717	0.900	0.789	0.914	0.918
MobileNetV3Large	224	0.837	0.863	0.799	0.875	0.830	0.912	0.917

ResNet-RS101	224	0.823	0.884	0.741	0.904	0.806	0.902	0.909
ResNet-RS200	224	0.823	0.879	0.745	0.899	0.807	0.903	0.906
EfficientNetV2B0	224	0.819	0.841	0.784	0.854	0.811	0.900	0.900
EfficientNetV2B1	240	0.831	0.847	0.806	0.856	0.826	0.904	0.909
EfficientNetV2B2	260	0.821	0.801	0.852	0.791	0.826	0.907	0.912
EfficientNetV2B3	300	0.825	0.873	0.758	0.891	0.811	0.908	0.913
EfficientNetV2S	384	0.844	0.867	0.810	0.878	0.837	0.914	0.919
EfficientNetV2M	480	0.835	0.853	0.807	0.863	0.830	0.915	0.919
EfficientNetV2L	480	0.832	0.839	0.819	0.845	0.829	0.909	0.906
ConvNeXtTiny	224	0.831	0.865	0.781	0.879	0.821	0.922	0.924
ConvNeXtSmall	224	0.827	0.866	0.772	0.882	0.816	0.918	0.922
ConvNeXtBase	224	0.830	0.834	0.820	0.839	0.827	0.910	0.913
ConvNeXtLarge	224	0.832	0.835	0.825	0.839	0.830	0.906	0.908
ConvNeXtXLarge	224	0.820	0.889	0.727	0.911	0.800	0.913	0.919
Vit-b16	224	0.822	0.816	0.828	0.816	0.822	0.906	0.909
Vit-b16_2	224	0.827	0.816	0.843	0.812	0.829	0.906	0.912

Vit-b16	320	0.811	0.863	0.736	0.885	0.794	0.905	0.909
Vit-b16	384	0.828	0.903	0.733	0.922	0.809	0.919	0.924
MLPMixerB32	224	0.817	0.856	0.759	0.874	0.804	0.901	0.898
MLPMixerB32_2	224	0.605	0.558	0.985	0.231	0.713	0.834	0.817
MLPMixerB32_3	224	0.768	0.716	0.884	0.653	0.791	0.864	0.862
Overall[b]		0.818±0.042	0.845±0.064	0.791±0.060	0.844±0.125	0.813±0.026	0.906±0.017	0.909±0.021
Ensemble model (Final model)		0.855	0.873	0.827	0.882	0.850	0.929	0.934
BNP Cut-off: 100 pg/ml (sub study)								
VGG16	224	0.838	0.843	0.915	0.703	0.877	0.915	0.952
VGG16	384	0.827	0.836	0.904	0.692	0.869	0.907	0.948
VGG19	224	0.838	0.852	0.902	0.728	0.876	0.913	0.951
VGG19	384	0.841	0.862	0.891	0.752	0.877	0.907	0.947
InceptionResNetV2	299	0.847	0.861	0.905	0.746	0.883	0.912	0.951
Xception	299	0.853	0.871	0.902	0.768	0.886	0.912	0.949

Xception_2	299	0.853	0.861	0.917	0.743	0.888	0.919	0.954
MobileNetV3Small	224	0.832	0.834	0.917	0.684	0.874	0.899	0.936
MobileNetV3Large	224	0.831	0.851	0.89	0.73	0.87	0.906	0.946
ResNet-RS101	224	0.828	0.845	0.892	0.716	0.868	0.891	0.93
ResNet-RS200	224	0.853	0.857	0.922	0.733	0.888	0.908	0.943
EfficientNetV2B0	224	0.837	0.859	0.889	0.748	0.874	0.898	0.936
EfficientNetV2B1	240	0.838	0.851	0.902	0.727	0.876	0.903	0.944
EfficientNetV2B2	260	0.842	0.864	0.892	0.756	0.878	0.908	0.946
EfficientNetV2B3	300	0.83	0.85	0.889	0.727	0.869	0.907	0.947
EfficientNetV2S	384	0.834	0.859	0.883	0.749	0.871	0.914	0.951
EfficientNetV2S_2	384	0.838	0.853	0.9	0.732	0.876	0.914	0.952
EfficientNetV2M	480	0.842	0.866	0.889	0.762	0.877	0.914	0.952
EfficientNetV2L	480	0.818	0.877	0.83	0.797	0.853	0.891	0.937
ConvNeXtTiny	224	0.815	0.837	0.88	0.701	0.858	0.886	0.927
ConvNeXtSmall	224	0.846	0.864	0.899	0.754	0.881	0.905	0.943
ConvNeXtBase	224	0.842	0.85	0.912	0.72	0.88	0.903	0.942

ConvNeXtLarge	224	0.825	0.867	0.855	0.773	0.861	0.89	0.931
Vit-b16	224	0.846	0.849	0.922	0.716	0.884	0.915	0.95
Vit-b16_2	224	0.831	0.849	0.891	0.725	0.87	0.907	0.944
Vit-b16	320	0.842	0.852	0.908	0.727	0.879	0.911	0.948
Vit-b16_2	320	0.822	0.816	0.929	0.636	0.869	0.899	0.938
Vit-b16	384	0.83	0.836	0.91	0.69	0.871	0.908	0.946
MLPMixerB32	224	0.843	0.88	0.871	0.794	0.876	0.907	0.948
MLPMixerB32_2	224	0.843	0.866	0.891	0.76	0.878	0.908	0.947
MLPMixerB32_3	224	0.838	0.851	0.903	0.725	0.876	0.906	0.945
Overall[b]		0.837±0.010	0.854±0.014	0.897±0.020	0.733±0.033	0.875±0.008	0.906±0.008	0.945±0.007
Ensemble model		0.853	0.867	0.909	0.759	0.888	0.921	0.956

AUC, area under curve; BNP, brain natriuretic peptide; PR, precision-recall curve; ROC indicates receiver-operating-characteristics curve.

[a] Model means the base-model of finetuning for the weak learners.

[b] Data was presented as mean ± standard deviation.

Prediction performance of elevated BNP level in the 100 images

	Accuracy	Sensitivity	Specificity
The AI model	0.920	0.880	0.957
The human participants	0.708±0.049	0.693±0.128	0.722±0.144

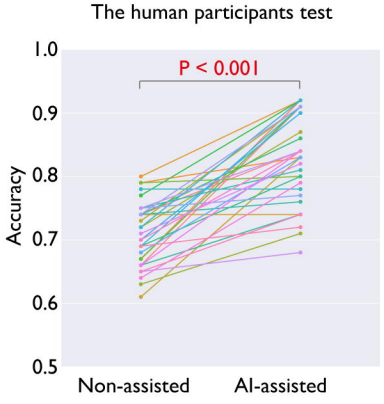

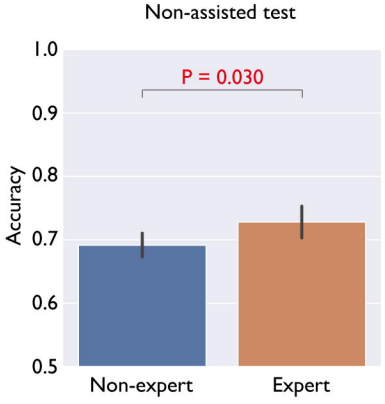

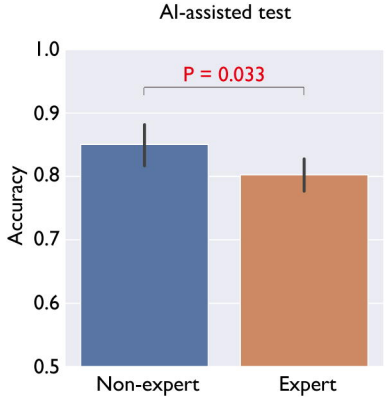

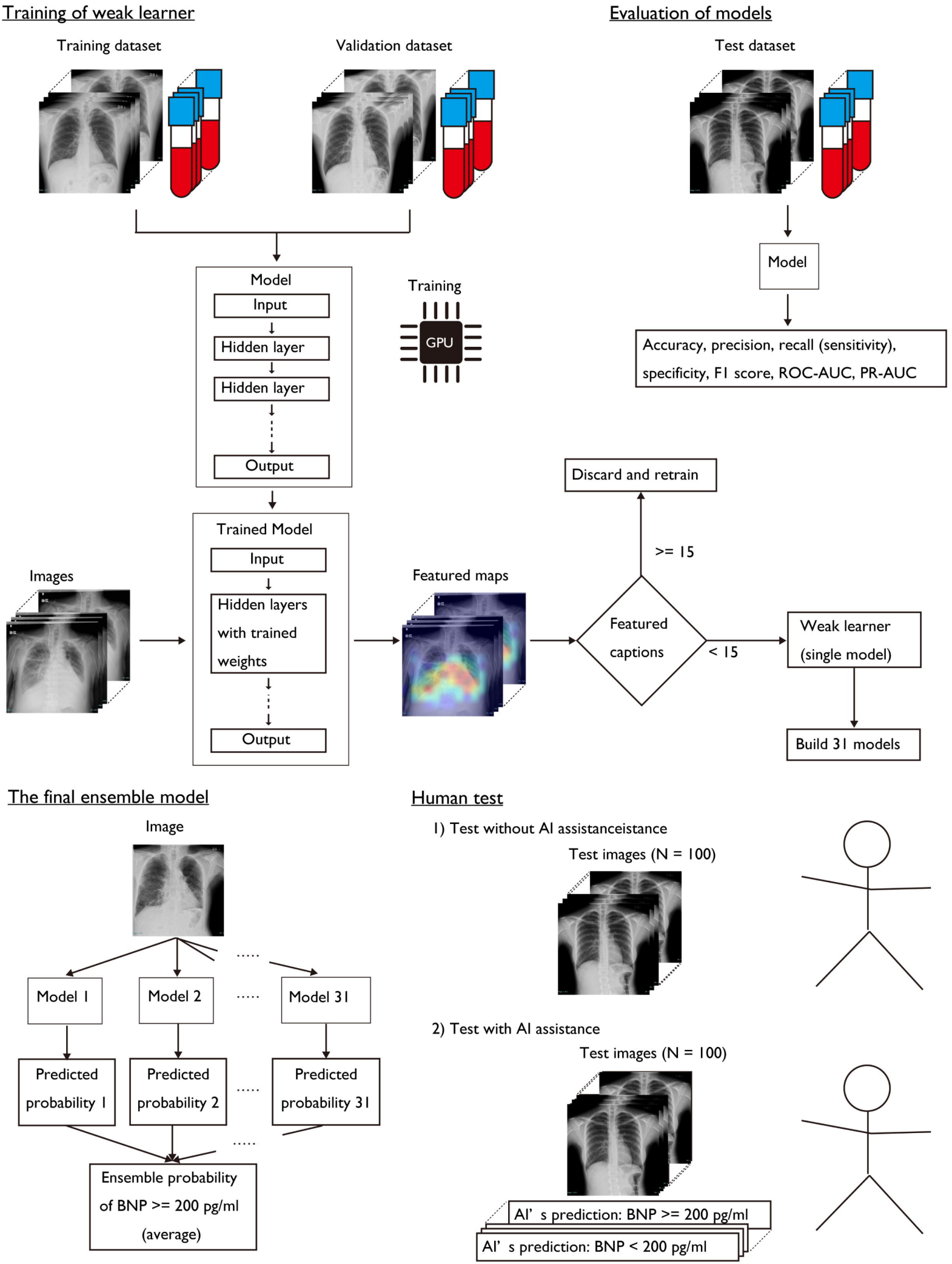
Training of weak learner
Training dataset
Validation dataset
Model
Input
Hidden layer
Hidden layer
Output
Training
GPU
Trained Model
Input
Hidden layers with trained weights
Output
Images
Featured maps
Discard and retrain
>= 15
Featured captions
< 15
Weak learner (single model)
Build 31 models
Evaluation of models
Test dataset
Model
Accuracy, precision, recall (sensitivity), specificity, F1 score, ROC-AUC, PR-AUC
The final ensemble model
Image
Model 1
Model 2
Model 31
Predicted probability 1
Predicted probability 2
Predicted probability 31
Ensemble probability of BNP >= 200 pg/ml (average)
Human test
1) Test without AI assistanceistance
Test images (N = 100)
2) Test with AI assistance
Test images (N = 100)
AI' s prediction: BNP >= 200 pg/ml
AI' s prediction: BNP < 200 pg/ml

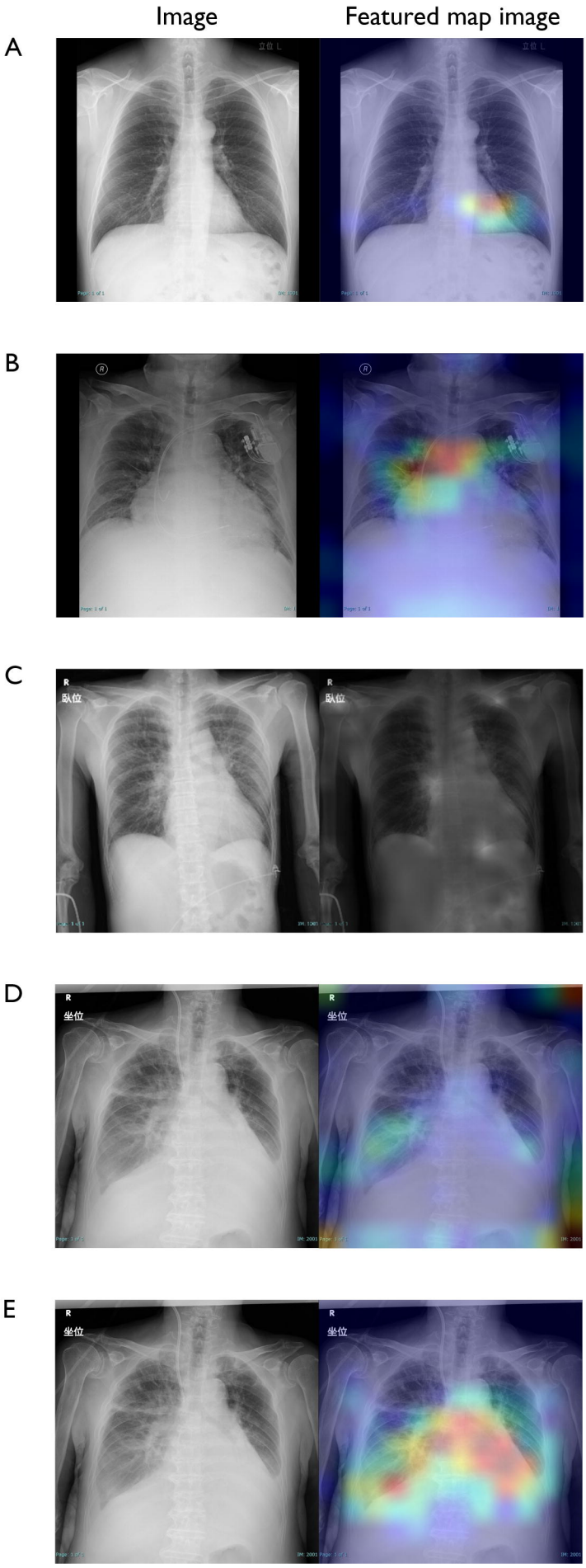
Image
Featured map image
A
B
C
D
E

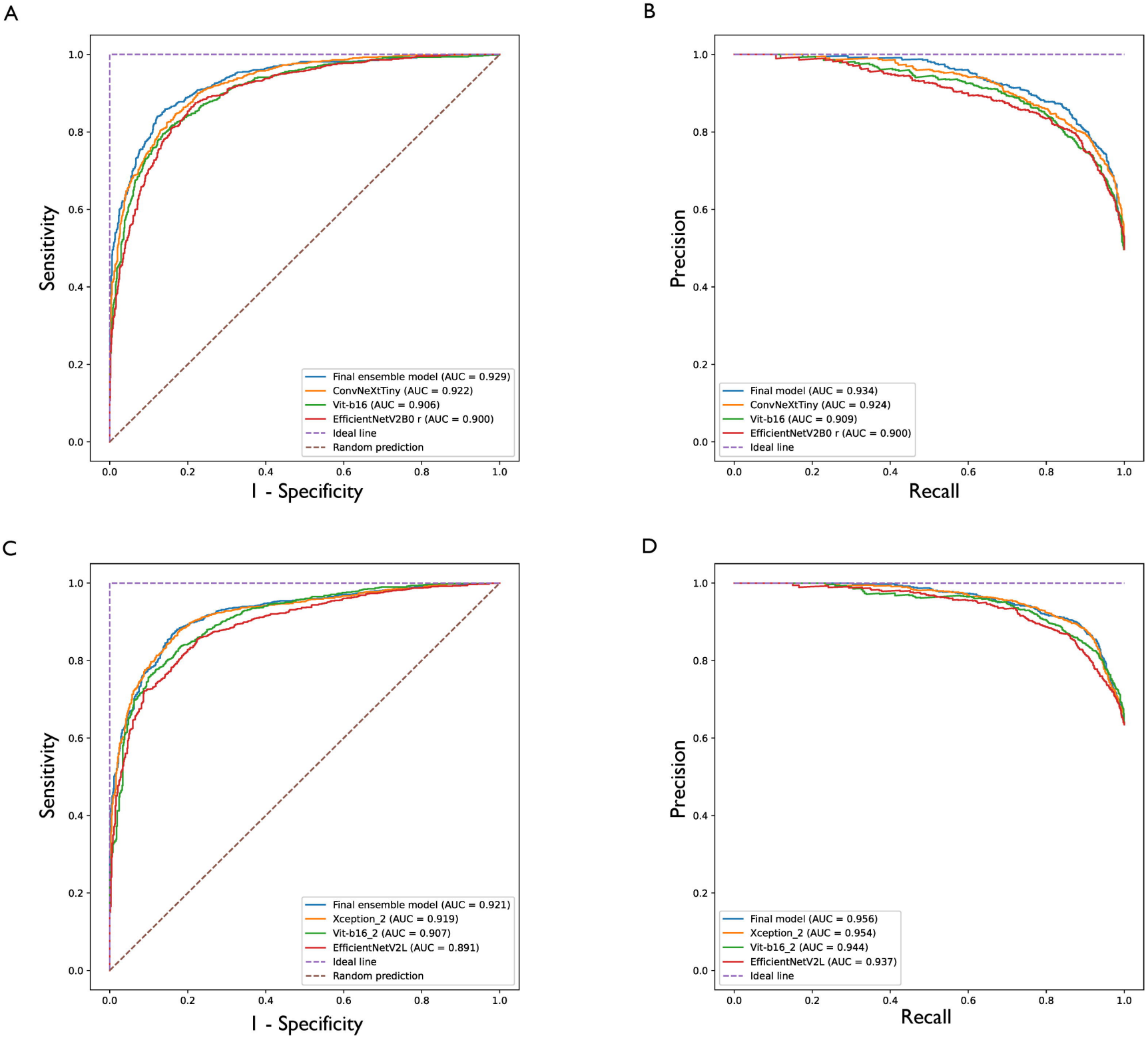
A
Sensitivity
1 - Specificity
Final ensemble model (AUC = 0.929)
ConvNeXtTiny (AUC = 0.922)
Vit-b16 (AUC = 0.906)
EfficientNetV2B0 r (AUC = 0.900)
Ideal line
Random prediction
B
Precision
Recall
Final model (AUC = 0.934)
ConvNeXtTiny (AUC = 0.924)
Vit-b16 (AUC = 0.909)
EfficientNetV2B0 r (AUC = 0.900)
Ideal line
C
Sensitivity
1 - Specificity
Final ensemble model (AUC = 0.921)
Xception_2 (AUC = 0.919)
Vit-b16_2 (AUC = 0.907)
EfficientNetV2L (AUC = 0.891)
Ideal line
Random prediction
D
Precision
Recall
Final model (AUC = 0.956)
Xception_2 (AUC = 0.954)
Vit-b16_2 (AUC = 0.944)
EfficientNetV2L (AUC = 0.937)
Ideal line

Image Featured map image

A

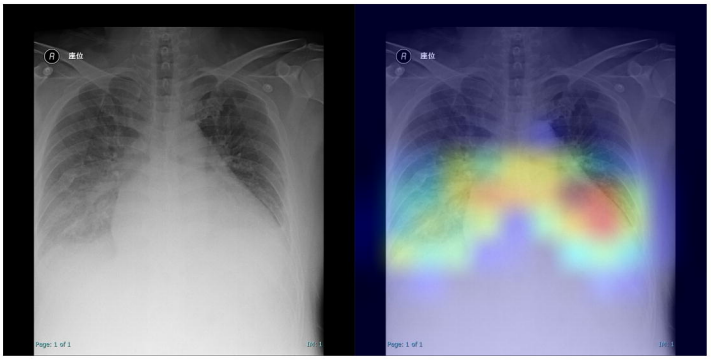

41 – 55 y.o. male

BNP 437 pg/mL

The AI prediction (BNP >= 200 pg/ml): 0.909

Humans' accuracy: 1.00

B

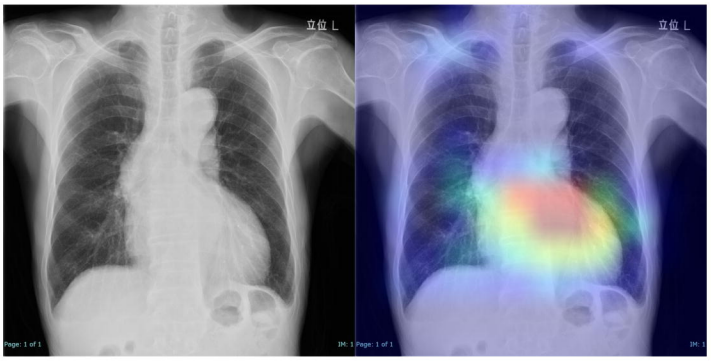

76 – 80 y.o. male

BNP 852 pg/mL

The AI prediction (BNP >= 200 pg/ml): 0.714

Humans' accuracy: 0.32

C

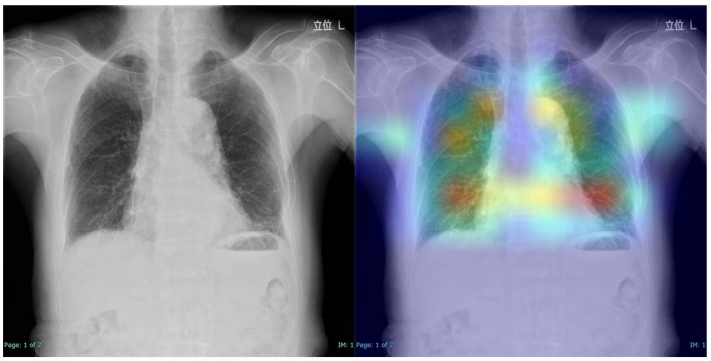

76 – 80 y.o. male

BNP 281 pg/mL

The AI prediction (BNP >= 200 pg/ml): 0.346

Humans' accuracy: 0.50

D

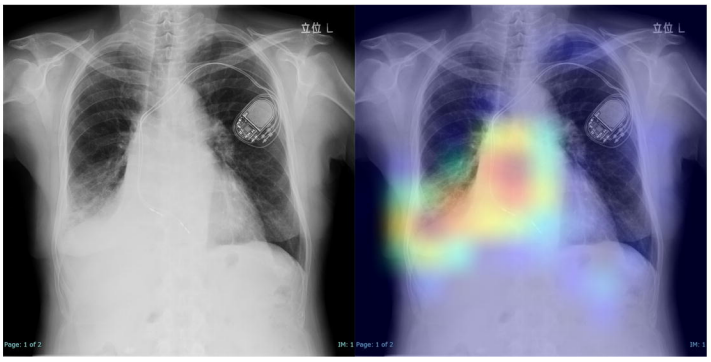

76 – 80 y.o. male

BNP 171 pg/mL

The AI prediction (BNP >= 200 pg/ml): 0.556

Humans' accuracy: 0.12

E

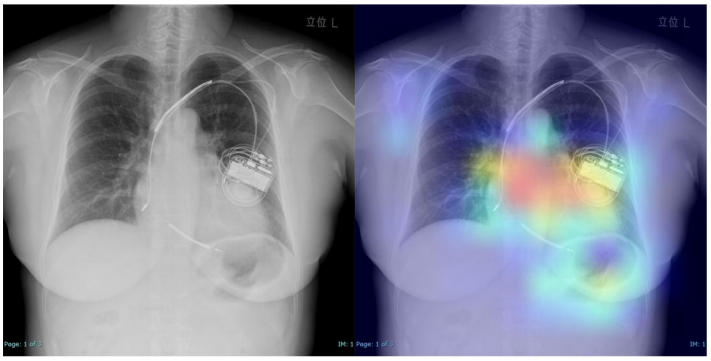

51 – 55 y.o. female

BNP 67 pg/mL

The AI prediction (BNP >= 200 pg/ml): 0.172

Humans' accuracy: 0.35

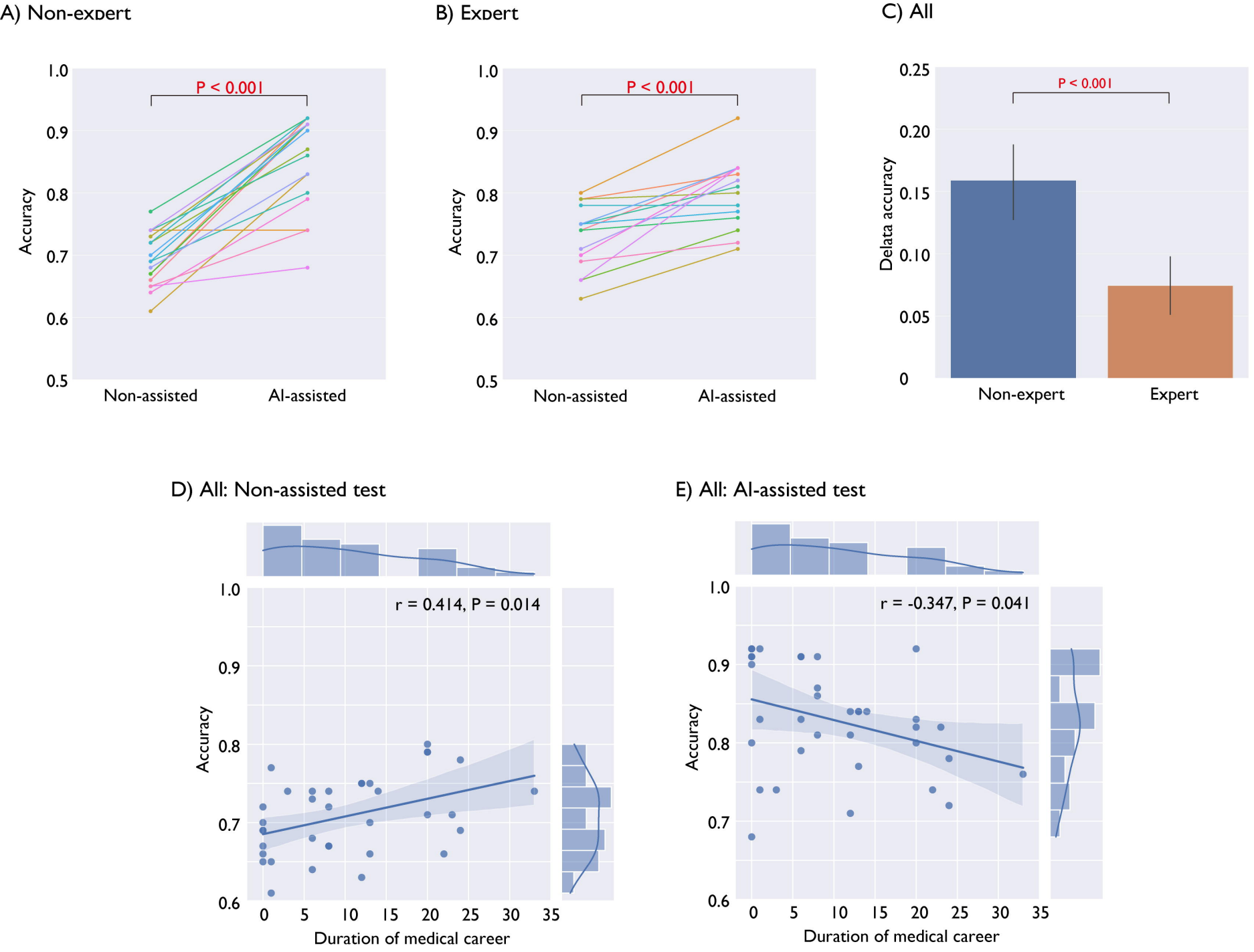
A) Non-expert
P < 0.001
Accuracy
1.0
0.9
0.8
0.7
0.6
0.5
Non-assisted
AI-assisted
B) Expert
P < 0.001
Accuracy
1.0
0.9
0.8
0.7
0.6
0.5
Non-assisted
AI-assisted
C) All
P < 0.001
Delata accuracy
0.25
0.20
0.15
0.10
0.05
0
Non-expert
Expert
D) All: Non-assisted test
r = 0.414, P = 0.014
Accuracy
1.0
0.9
0.8
0.7
0.6
0
5
10
15
20
25
30
35
Duration of medical career
E) All: AI-assisted test
r = -0.347, P = 0.041
Accuracy
1.0
0.9
0.8
0.7
0.6
0
5
10
15
20
25
30
35
Duration of medical career